X-ray Diffraction and Raman Spectroscopic Studies of Glasses and Glass-Ceramics Inside the A_2O-MoO_3-Nb_2O_5-P_2O_5 (A= Li, Na) Systems

H. Bih[1], L. Bih[1*], M.P.F. Graça[2], M.A. Valente[2] and B. Elouadi[3]

[1] Equipe Sciences de Matériaux, FST-Errachidia, Maroc
[2] Physics Department (I3N), Aveiro University, Campus Universitário de Santiago, 3810 – 193, Aveiro – Portugal
[3] University of the La Rochelle, France

Abstract

Phosphate glasses in the system (50-x)A_2O-xMoO_3-10Nb_2O_5-40P_2O_5 (AMo-40), with x=0; 30 and A=Li or Na were prepared by the melt quenching method. The effect in the crystallization behaviour of the glass due to the introduction of MoO_3 in the glass composition and varying the molar ratio between network modifiers and network formers (M/F) was studied. The prepared glasses were heat-treated in air, at 550, 600 and 650 ºC for 4 hours. The structure, of the obtained samples, was studied by differential thermal analysis (DTA), X-ray powder diffraction (XRD), Raman spectroscopy and the morphology by scanning electron microscopy (SEM). It was found that the replacement of Li_2O or Na_2O by MoO_3 reduces the number of the crystallised phases. In the lithium-niobiophosphate glasses the presence of MoO_3 promotes the formation of $NbOPO_4$ and reduces the formation of ortho- and pyro-phosphate phases. The thermal treatments affect the arrangements of the network structure of the AMo-40-glasses.

Introduction

Phosphate glasses are important materials in technologically comparing with the conventional oxide glasses. They possess some superior physical properties such as high thermal expansion coefficients, low melting temperature, low softening temperatures and smaller liquids viscosity than silicate glasses. Another important feature of these glasses is their ability to incorporate large amounts of transition metal without reduction of glass forming ability. These properties make them useful candidates for fast ion conducting material and other important applications such as laser hosts, nuclear waste glasses, glass-to-metal seals and bio-compatible materials [1]. However, their relatively poor chemical durability makes them generally unsuitable for practical applications [2]. It was suggested [3-5] that the addition of one or more oxides such as SnO, PbO, ZnO, CuO, Al_2O_3, Fe_2O_3, etc., have been observed to be good stabilizers of phosphate glasses and these oxides are expected to improve the physical properties to a considerable extent and thereby enhance the range of applicability of these glasses.

Transition and rare-earth ions containing oxide glasses have attracted much attention because of their semiconducting properties and potential applications in optical devices such as solid-state lasers and optical fibers for communications [6-9]. Due to the fact that some phosphate glasses showed alkali ion conductivities even at room temperature, since these glasses possess more open structure for ionic transport, they are being studied extensively over the last decade in order to be applied in energy storage devices and solid-state batteries [10-13]. Recently [14], lithium phosphoniobate glasses belonging to the system Li_2O-Nb_2O_5-P_2O_5 (LNP) glasses have shown that their electric transport is due only to lithium ion conductivities and no electron transfer was detected. More recently [15], these glasses doped with tungsten ions (LNPW) showed mixed ionic-electronic conductivity and may be used as positive electrodes in solid-state batteries.

*corresponding author. Email: bihlahcen@yahoo.fr

 Printed in Kazakhstan

Tungsten oxide presents several interesting optical properties such as electrochromic [16-18], photochromic [16, 17, 19], and thermochromic [20, 21] properties, which are known for provoking a color change due to the action of an electric field, electromagnetic radiation and heat, respectively. These properties have been widely studied and it has been found that they are due to the fact that tungsten atoms have the ability to adopt various oxidation states. Therefore, several applications have appeared for such oxides including sensors of gases and of humidity, electronic information displays, photoelectric sensors or smart windows [22]. Since chemical properties of tungsten and molybdenum are very similar in condensed matter, MoO_3-based glasses should exhibit such interesting properties.

The present work is in continuation of our earlier work [14] on Li^+ ion conduction and thermal crystallization characteristics in different phases of lithium niobium phosphate systems. The addition of MoO_3 to the above investigated Li_2O-Nb_2O_5-P_2O_5 system [14] has been taken up for investigation.

Experimental measurements

Glass samples of composition $40P_2O_5$-$20A_2O$-$10Nb_2O_5$-$30MoO_3$ (A = Li, Na) (mol %) were prepared using as starting materials reagent grade chemicals A_2CO_3, $(NH_4)H_2PO_4$, Nb_2O_5 and MoO_3. More details are given elsewhere [14]. In order to obtain glass-ceramics, specimens of the glass samples were heat treated with a rate of 4°C/min from the room temperature to different temperatures above the glass transition temperature in air. They were maintained at the treatment temperature for 2 hours, and then were slowly cooled in the furnace down to the room temperature. The structural, thermal, electrical conductivity properties of the samples were analyzed by means of different techniques.

Results

XRD, density, molar volume and DTA studies

The glassy samples prepared as mentioned in the experimental part were homogeneous and transparent. The density is equal for the glasses (d=2.96), whereas the molar volume of the sodium based glass (V_m=44.05 cm^3) is higher than that of LiMo-40 glass (V_m=40.97 cm^3). Increase in the molar volume suggests that the glassy matrix becomes more open for Na-based glass in agreement with the increase of the alkali size radius in the order Na>Li.

DTA curves for AMo-40 (A = Li, Na) glasses, measured with a heating rate of 10 K/min are similar and show two exothermic peaks at 550°C and 640°C. By comparing the DTA spectrum of the mother glass (Li-40) ($40P_2O_5$-$50Li_2O$-$10Nb_2O_5$ (% mol)) [14] with the spectra of LiMo-40 and NaMo-40 we state that the introduction of the MoO_3 oxide into the glass-network, where the P_2O_5 and Nb_2O_5 molar ratio is kept constant, induces deep changes in the thermal properties. One can note that the Tg value for the glass LiMo-40 (Tg= 289°C) is lower than that of Li-40 (Tg= 450°C) [14]. By considering that the partial replacement of Li_2O by MoO_3 is associated with the increase of O/P ratio (from 3.75 to 4.25), it is possible to correlate the observed decrease of the glass transition temperature to the enhancement of the depolymerisation of the network. The obtained results show that very large difference between the Tg and Tc temperatures (about 260 °C) is observed for both the AMo-40 glasses. This result points to stability of them.

X-ray diffraction and SEM micrographs

Fig.1 shows XRD patterns of the crystallized samples by heat treatment at different temperatures. The annealing of samples was performed at temperatures below and above the characteristic points shown in DTA curves in order to identify a structure that appears in X-ray patterns of the annealed samples. In addition to an amorphous phase the XRD patterns show the formation of some crystalline phases. The resulting crystalline phases were characterized by X-ray diffraction and compared with diffraction patterns of known crystalline compounds containing Li, Na, P, Nb, Mo and O using database PDF2.

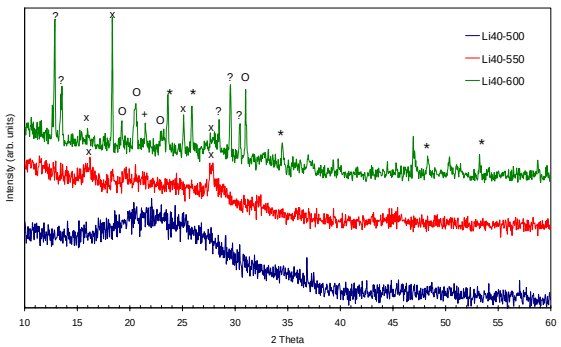

Fig. 1. X-Ray diffraction patterns of the LiMo-40 glass submitted to different heat-treatments

This investigation shows that the heat-treatments of LiMo-40 induce the formation of several crystalline phases ($LiPO_3$, $Li_4P_2O_7$, Li_3PO_4, $LiNbO_3$ and unknown phase). It is worth to mention that the same crystalline phases were formed by heat-treatment of the mother glass (Li-40) [14]. According to this result, it seems that the replacement of Li_2O by MoO_3 neither reduces the number of the alkali-phosphate crystalline phases in the glass-ceramics nor prevents the formation of the unknown phase. On the contrary, the replacement of Na_2O by MoO_3 shows that only diffraction peaks associated with the $NbOPO_4$ phase were detected in XRD patterns of NaMo-40 submitted to heat-treatments. In the AMo-40 (A = Li, Na) glasses, the O/P ratio is 4.25, so the network structure is expected to be dominated by orthophosphate Q^0 groups. In agreement with the structural O/P ratio, the XRD patterns show the formation $NbOPO_4$ structure, in the NaMo-40 samples treated at 550°C and 650ºC, which consists of Q^0 units sharing corners with niobium NbO_6 units. The formation of such phase in Na-based samples suggests that the crystallisation of NaMo-40 glass involves the chemical reaction between phosphate (PO_4) and niobate (NbO_6) units while all Na^+ ions remain in the amorphous state. Therefore, the nature of the alkaline influences the structure of the AMo-40 (A = Li, Na) glass-ceramics.

The SEM micrographs (Fig.2) of the LiMo-40 and NaMo-40 samples treated at different temperatures revealed the presence of particles with different shapes in both compositions.

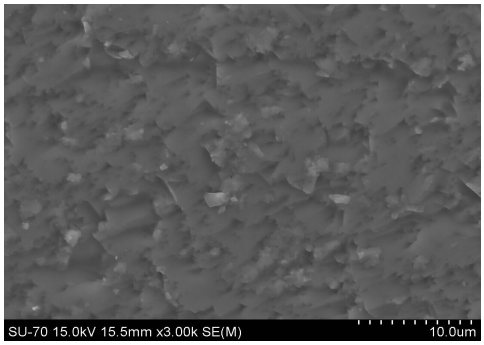

Fig. 2. SEM micrographs of the LiMo-40 submitted to heat treatment for 4hours at 550°C

According to the X-Ray investigation, these particles could be associated with alkali-phosphate and/or lithium niobate phases. The crystallization of a glass upon heating is a complex mechanism which depends on kinetic and thermodynamic parameters such as diffusion coefficient, molar volume, free energy and interfacial energy between crystalline and glassy phase. Crystallization in glasses is generally classified as surface or internal crystallization depending if the crystalline phase grows from the surface or from nuclei inside the bulk. However, these two processes often occur simultaneously and competitively but one of them will be dominant and will define the crystallization process [23, 24].

Raman spectroscopy

Fig.3a and Fig.3b show Raman spectra of the LiMo-40 and NaMo-40 as-prepared glasses in addition to the spectra of these glasses after they have submitted to different heat-treatments for different period of times, respectively. In curves Li40-base and Na40-base of Fig.3a and Fig3b, respectively, one has to note that the spectra are almost similar suggesting the presence of analogous structural units in their networks. The main peaks around 1230, 950, 400 and 260 cm^{-1} are predominant in each spectrum. The bands present some broadening effect which is characteristic of the glass structure. Vibrations related with the NbO_6 octahedral (226, 260, 335, 400, 610 cm^{-1}), stretch of PO_4^{3-} units (950 cm^{-1}), PO_2 anti-symmetric vibrations (1230 cm^{-1}) were detected.

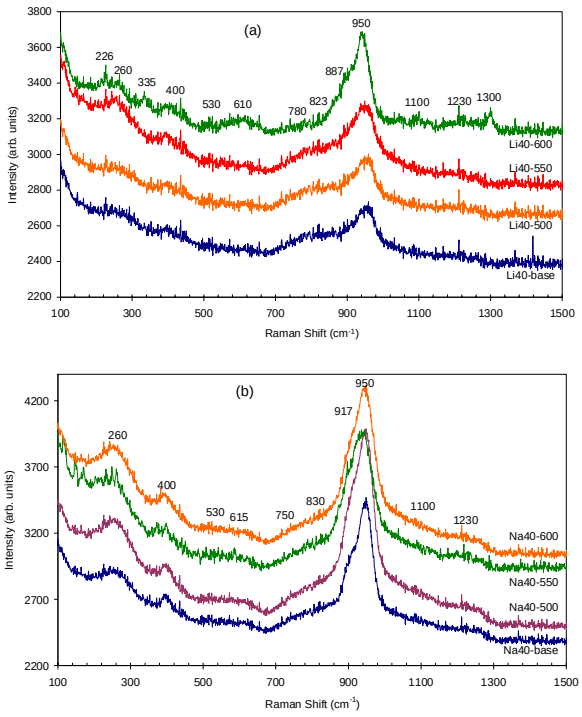

Fig. 3. Raman spectra of: (a) LiMo-40 and (b) NaMo-40 base-glasses submitted to heat-treatments at different temperatures

The assignments of Raman spectra of the AMo-40 samples is made on the basis of the assignments of Raman spectra for the $Li_2O–P_2O_5$ glass [25]: the bands at around 600–760 cm^{-1} are due to P–O–P (bridging oxygen) stretching modes; the Raman bands in the region from 900 to 1300 cm^{-1} are associated with stretching vibrations of Q^3, Q^2, Q^1 and Q^0 species, where n in the Q^n terminology represents the number of bridging oxygens (BO) per (PO_4) tetrahedron. In a Li-40 glass-ceramic the most observed peaks were at 1300 cm^{-1} ($\upsilon_{as}P=O$), 1100 cm^{-1} ($\upsilon_s(PO_2)^-$), 1050 cm^{-1} ($\upsilon_s(PO_3^{2-})$, 950 cm^{-1} ($\upsilon_s(PO_4^{3-})$), 905 cm^{-1} (υ_s(Nb–O)), 735 cm^{-1} (υ_s(P–O–P)), 657 and 605 cm^{-1} ($\upsilon(NbO_6)$), 420-225 cm-1 (υ (NbO_6), and 186 cm^{-1} ($\delta(PO_4)$). According to our Raman investigation, the same modes with changes of the intensity and/or the position are observed for LiMo-40 glass-ceramic. The peaks lying in the range frequency 600-700 cm^{-1}, assigned to the symmetric P-O-P stretching vibration [ν(P–O–P) sym] of the symmetric PO_2 units, are weak. Low intensity of the PO_2 anti-symmetric vibrations (1230 cm^{-1}) is also seen from the Raman spectra. The low intensity of these phosphate modes suggests the presence of low content of chain-like phosphate structures in their glassy-matrix. The broad band around 610-615 cm^{-1} could be ascribed to the vibrations of elongation ν_s(POM) (M = Nb, Mo). The band around 530 cm^{-1} is probably connected to the vibrations of phosphate units deformation. Lastly, the components located in the frequency range 100-400 cm^{-1} are associated with the deformation modes of (MO_6) and or (PO_4) units.

The Raman spectrum of Li40-500°C is almost similar to that of Li40-base (Fig. 3a) suggesting that the effect of this heat-treatment do not induces any new vibrational modes. However, one can note that the heat-treatments at 550°C and 600°C decrease the intensity of a broad band at 780-823 cm^{-1} and promote the appearance of new bands at 1100 cm^{-1}, 1300 cm^{-1} and around 610 cm^{-1}. The spectrum Li40-600°C of Fig.3a shows clear decreases of the intensity of the band located in the 780-823 cm^{-1} frequency region. The position and the intensity of a band at 880 cm^{-1} remain unchanged and this vibration mode has been previously assigned to a vibrational of Nb–O in octahedral NbO_6 or Nb–O–P linkage [26]. From the comparison of the Raman spectra of Na40-600°C, Na40-500°C, Na40-550° with that of Na40-base (Fig.3b), one can observe that the intensity of a broad band 750-830 cm^{-1} is not changed and the effect of the heat-treatment contributes only to the increase of the intensity of a shoulder located at 917 cm^{-1}.

Discussion

Raman spectra of studied glasses are shown in Fig. 3. It can be noticed that the Raman bands of the AMo-40 glass are observed in a similar wavenumber regions. This suggests that the glass network contains the same structural units. However, the intensity and the position of the Raman bands for the crystallised LiMo-40 and NaMo-40 glasses are different (Fig.3). The presence of Raman bands near 335, 610, 1100 and 1300 cm^{-1} in LiMo-40-600°C, which were not observed in the NaMo-40-600°C and which can be assigned to vibration modes of phosphate units, indicates that the LiMo-40 glass-ceramic structure contains large amount of phosphate groups. On the other hand, similarities exist between the spectra of the glass-ceramics LiMo-40 and Li-40 (MoO_3-free glass) [14]. Considering the chemical compositions of the glasses, the calculated [O]/[P] ratio are 3.75 and 4.25 for the MoO_3-free glass and for the AMo-40 glasses, respectively. According to this [O]/[P] criterion, it is expected that the AMo-40 structures will contain mainly orthophosphate groups (Q^0) since the O/P ratio is equal to 4.25. This expectation is confirmed by the Raman spectroscopy since band relative to orthophosphate (950 cm^{-1}) vibration mode is the most intense feature seen in Fig.3. It is worth to note that the most intense Raman band near 950 cm^{-1} can be also unambiguously assigned to symmetric stretching mode of MoO_6 units.

The crystallisation of LiMo-40 glass does not promote the preparation of glass-ceramics with only $LiNbO_3$ crystallites (Fig.1) in agreement with the Raman spectra of the heat-treated samples which showed the 950 cm^{-1} (Li_3PO_4), 1050 cm^{-1} and 1100 cm^{-1} ($Li_4P_2O_7$), and 1230 cm^{-1} ($LiPO_3$) vibration modes. On the contrary, the heat-treatments of NaMo-40 glass transform it to glass-ceramic containing $NbOPO_4$ phase. The crystalline $NbOPO_4$ corresponds to octahedral chains [NbO_6] parallel with the c-axis. These chains are connected between them by tetrahedrons [PO_4] to form a three dimensional structure; these corner sharing polyhedrons [NbO_6] do not have terminal oxygen ions but they are distorted, giving an alternation of short and long bonds [27] and the Raman spectrum of this phase showed a band near 800 cm^{-1}. The analysis of the Raman spectra of AMo-40 samples

(Fig.2a, 2b) shows clearly that some bands appear in the frequency range 800-920 cm^{-1}. Shannon et al. [28] clearly highlighted the displacement of the bands towards higher frequencies when the degree of distortion of octahedral increases but also when the number of terminal bonds Nb-O_T pointing towards modifying ions grows. Therefore, the bands observed around 900-917 cm^{-1} can be ascribed to the distorted [NbO_6] octahedral having at least a short Nb-O bond pointing towards a modifying ion. The bands seen in the range near 823-830 cm^{-1} could be associated to the Nb-O vibrations in distorted octahedral which can present an association by their corners with at least another octahedra of niobium. The emergence of broad band near 750-780 cm^{-1} can be explained by the presence in the glass matrix of the Nb-O vibration in less distorted NbO_6 octahedral. Generally, the presence of bands below 790 cm^{-1} suggests the existence of less distorted octahedral units [29].

From the XRD and Raman investigations carried out on the AMo-40 (A = Li, Na) materials, it is assumed that a mixture of phases and $NbOPO_4$ are issued from the crystallisation of LiMo-40 and NaMo-40 glasses, respectively. One question arises here, why the number of phases in the glass-ceramics AMo-40 (A= Li, Na) depends on the nature of the alkaline ions? The crystallization of a glass upon heating depends on kinetic and thermodynamic parameters such as diffusion coefficient, molar volume, free energy and interfacial energy between crystalline and glassy phase. Crystallization in glasses is generally classified as surface or internal crystallization depending if the crystalline phase grows from the surface or from nuclei inside the bulk. However, these two processes often occur simultaneously and competitively but one of them will be dominant and will define the crystallization process. We can note that the heat treatments of the LiMo-40 glass which is associated with a surface crystallisation process could be at the origin of the formation of highly basic lithium phosphates and $LiNbO_3$ phase in LiMo-40 glass-ceramics. Thus, the LiMo-40 glass is unstable at high temperature and separate into different phases in the superliquid state. In spite of this phase separation, the NaMo-40 glass can be crystallized easily to yield single phase NbOPO4 but this crystallization must be performed in the range of about 550-600°C. The observed differences in the crystallization behaviour of the studied glasses can be most likely attributed to differences in viscosity of the melts and stability of different crystalline phases due to significant differences in ionic size of alkali metal ions.

Conclusions

DTA, XRD, SEM and Raman studies have been performed for LiMo-40 and NaMo-40 glasses of the composition corresponding to $40P_2O_5$-$20A_2O$-$10Nb_2O_5$-$30MoO_3$ (A = Li, Na) (mol %). These studies showed that the main structural units of the network are orthophosphate groups. These glasses contain, however, also some smaller amount of metaphosphate and pyrophosphate units. Our results pointed out that the AMo-40 glasses present good thermal stability. It is, therefore, very likely that it will be possible to control the extent of the crystallization obtaining transparent nanostructured samples by means of proper heat treatment. The LiMo-40 glass is however unstable at high temperature and separate into different phases in the superliquid state. In spite of this phase separation, the NaMo-40 glass can be crystallized easily to yield single phase NbOPO4 but this crystallization must be performed in the range of about 550-600°C. The observed differences in the crystallization behavior of the studied glasses can be most likely attributed to differences in viscosity of the melts and stability of different crystalline phases due to significant differences in ionic size of alkali metal ions.

Acknowledgment

The authors express their gratitude to CNRST (Morocco-FCT (Portugal) for financial support to this work.

References

1. P.Y. Shih, Mater. Chem. Phys. 84 (2004) 151.
2. M.R. Reidmeyer, M. Rajaram, D.E. Day, J. Non-Cryst. Solids 85 (1986) 186.
3. C.M. Shaw, J.E. Shelby, Phys. Chem. Glasses 29 (1988) 87.
4. I.W. Donald, J. Mater. Sci. 28 (1993) 2841.
5. R.K. Brow, R.J. Kirkpatrick, G.L. Turner, J. Am. Ceram. Soc. 73 (1990) 2293.
6. J.D. Mackenzie, in: J.D. Mackenzie (Ed.), Modern Aspects of the Vitreous State, vol. 3, Butterworth, London, 1964, p. 126.
7. N.F. Mott, J. Non-Cryst. Solids 1 (1968) 1.
8. D. Adler, Amorphous Semiconductors, CRC, Cleveland, OH, 1971.

9. I.G. Austin, E.J. Garbett, in: P.G. LeComber, J. Mart (Eds.), Electronic and Structural Properties of Amorphous Semiconductors, Academic Press, London, 1973, p. 393.
10. F. Borsa, D.R. Torgeson, S.W. Martin, H.K. Patel, Phys. Rev. B 46 (1992) 795.
11. B.V.R. Chowdari, K.F. Mok, J.M. Xie, R. Gopalakrisnan, Solid State Ionics 76 (1995) 189.
12. R. Winter, K. Siegmund, P. Heitjans, J. Non-Cryst. Solids 212 (1997) 215.
13. T. Takahashi, High Conductivity Solid Ionic Conductors, Recent trends and applications, World Scientific Publishers, 1989.
14. M.P.F. Graça, M.A. Valente, M.G. Ferreira da Silva, J. Mat. Sci., 41 (2006) 1137.
15. M.P.F. Graça, M.A. Valente, H. Bih, L. Bih, J. Non-Cryst. Solids, accepted.
16. C. Bechinger, M.S. Burdis, J.G. Zhang, Solid State Commun. 101 (1997) 753.
17. J. Scarminio, Sol. Energy Mater. Sol. Cells 79 (2003) 357.
18. X.G. Wang, Y.S. Jang, N.H. Yang, Y.M. Wang, L. Yuan, S.J. Pang, Sol. Energy Mater. Sol. Cells 63 (2000) 197.
19. C. Bechinger, D. Ebner, S. Herminghaus, P. Leiderer, Solid State Commun. 89 (1994) 205.
20. S.M.A. Durrani, E.E. Khawaja, M.A. Salim, M.F. Al-Kuhaili, A.M. Al- Shukri, Sol. Energy Mater. Sol. Cells 71 (2002) 313.
21. K.R. Padmanabhan, Nucl. Instrum. Methods Phys. Res., Sect. B 219 (2004) 942.
22. S.K. Deb, Philos. Mag. 27 (1972) 801.
23. D.R. Uhlmann, Mater. Sci. Res. 4 (1969) 172.
24. G.W. Scherer, Mater. Sci. Technol. 9 (1991) 119.
25. R. K. Brow, J. Non-Cryst.Solids, 263/264 (2000) 1.
26. A. El Jazouli, R. Brochu, J.C. Viala, R. Olazcuaga, C. Delmas, G. Le Flem, Ann. Chim. Fr. 7 (1982) 285–292.
27. A.A. Mc. Connel, J.S. Anderson, G.N.R. Rao, Spectrochim. Acta, 32A (1976) 1067.
28. R.D. Shannon, Acta Cryst. A, 32 (1976) 751.
29. K. Fukumi et S. Sakka, J. Mater. Sci., 28 (1988) 4305.

Received 17 March 2010